Lattice polarisation around off-centre Li in $Li_xK_{1-x}TaO_3$

1990 J. Phys.: Condens. Matter 2 4341

(http://iopscience.iop.org/0953-8984/2/19/003)

J. Phys.: Condens. Matter **2** (1990) 4341–4350. Printed in the UK

Lattice polarisation around off-centre Li in $Li_xK_{1-x}TaO_3$

M G Stachiotti and R L Migoni
Instituto de Fisica Rosario, Universidad Nacional de Rosario, 27 de Febrero 210 Bis, 2000 Rosario, Argentina

Received 5 July 1989, in final form 19 December 1989

Abstract. The off-centre displacement δ of a Li ion in $KTaO_3$ and the surrounding lattice distortion is calculated using a non-linear shell model developed for the pure lattice. The method of the static lattice Green function is applied and the range of the Li dipole forces is limited to a few lattice constants. A short-range Li–O interaction potential is used which leads to a lithium displacement in reasonable agreement with estimations made from NMR measurements. A lattice polarisation is found to develop in a region around the Li, whose total dipole moment exceeds by a factor of 4.5 that arising from the Li displacement itself. This is in satisfactory agreement with the observed dielectric properties. The shape of the polarised region is strongly anisotropic, the longer axis being coincident with the (incipient ferroelectric) polar axis.

1. Introduction

Studies of ordering in crystals containing off-centre impurities have led to a new line of research after the discovery [1] in 1974 that Li is an off-centre ion when it substitutes for K in the highly polarisable dielectric $KTaO_3$. Potassium tantalate is a cubic paraelectric perovskite which shows a ferroelectric soft mode and becomes nearly unstable when approaching 0 K. The Li^+ impurity replacing the K^+ ion has, because of its smaller ionic radius, a position shifted along a $\langle 100 \rangle$ direction relative to the crystal lattice site [2, 3]. The Li displacement has been estimated from NMR measurements of the quadrupole-coupling frequency [2, 4] using a model of polarisable point charges at ideal sites [5]. A δ-value of $0.32a$, where a is the lattice constant, has been obtained. Dielectric relaxation [6], pyroelectric [7] and ESR [8] measurements indicate that the dipole moment associated with each Li impurity exceeds by about one order of magnitude the value corresponding to the above displacement. These results have been interpreted in terms of a 'cluster' of polarised lattice ions around the impurity.

At low Li concentrations (i.e. below about 2%), when the clusters presumably do not interact, their polarisations are randomly oriented along the six equivalent Li displacements. Relaxational dynamics between the equivalent cluster configurations have been observed [2]. Below a concentration-dependent temperature T_g the dipoles freeze into a glass-like polar phase analogous to a magnetic spin glass [4, 6].

At higher concentrations and low temperatures, whether the system undergoes a transition to a dipole glass or a ferroelectric phase is still under discussion [9, 10].

A theoretical description of the phenomena observed in $Li_xK_{1-x}TaO_3$ can be attempted on the lines of the spin-glass theory. However, a complication does arise

0953-8984/90/194341 + 10 $03.50

for dipoles owing to the modification of their interaction by the lattice polarisation. Moreover, even a knowledge of the effective dipole magnitude is insufficient information since the interaction potential obviously depends on the shape of the polarised clusters.

The lithium displacement has been previously calculated [5] minimising the potential energy in a model where all ions are represented as point-polarisable point charges and assumed to be fixed at their ideal positions except for a single Li^+ ion, which is allowed to move along a $\langle 100 \rangle$ direction. A value of δ in good agreement with that determined from NMR measurements has been found. However, the permanent dipole created by the off-centre Li ion is nearly completely screened by the induced dipole moments in the host lattice.

The purpose of the present paper is to perform a more realistic calculation of the Li^+ and surrounding crystal configuration in the framework of a model which allows ionic displacements as well as electronic polarisation. A non-linear shell model is applied which has given a satisfactory description of the lattice dynamics of $KTaO_3$ in a wide range of temperatures [11]. The lattice distortion around an isolated Li^+ impurity is calculated self-consistently, together with δ, by the Green function method.

2. Model and formulation of the calculus

For the pure lattice we use a model which allows us to describe the lattice dynamics and ferroelectric behaviour in oxidic perovskites ([12] and references therein). In particular the model gives a very accurate description of the dynamical properties of $KTaO_3$ [11]. It includes axially symmetric short-range forces which couple the shell of each oxygen ion to those of its nearest K^+, Ta^{5+} and O^{2-} ions. Both the K^+ and the Ta^{5+} ions are considered to be isotropically polarisable, each with a shell charge Y and a core–shell coupling constant K. However, since the oxygen polarisability depends strongly on its crystal environment, two independent core–shell force constants are considered for this ion: K_{OB} for core–shell displacements directed towards its neighbouring Ta^{5+} ions and K_{OA} for those lying in the plane where the oxygen is surrounded by four K neighbours (figure 1). The model includes a fourth-order anisotropic interaction K_{OB-B} at the oxygen ion, for relative core–shell displacements along the direction of its neighbouring Ta^{5+} ion. This fourth-order interaction is treated for the pure crystal in the self-consistent phonon approximation (SPA), leading to an effective harmonic core–shell coupling $K_{OB}(T)$ [11, 12]. The bare harmonic model is unstable, and the crystal is only stabilised in the paraelectric phase through the anharmonic term of the potential. Therefore, in order to perturb a stable crystal with the defect, we shall consider the effective coupling to be the harmonic core–shell coupling at the oxygen.

When a K^+ ion of the pure $KTaO_3$ crystal is substituted by an off-centre Li^+ ion, the surrounding lattice (in the static approximation) distorts in order to minimise the potential energy. This can be decomposed as the sum of the pure crystal potential ϕ and a defect potential $V = V_{Li} - V_K$. Clearly we understand by 'defect' the Li^+ ion at the off-centre position together with the vacant K^+ ion. V_{Li} includes short-range and Coulomb interactions between the Li^+ ion and the host lattice cores and shells with the exclusion of the vacant K^+ ion, while $-V_K$ cancels the same types of interaction arising from the K^+ ion eliminated from the centrosymmetric position. Except for the previously mentioned fourth-order interaction, the remaining short-range and Coulomb inter-

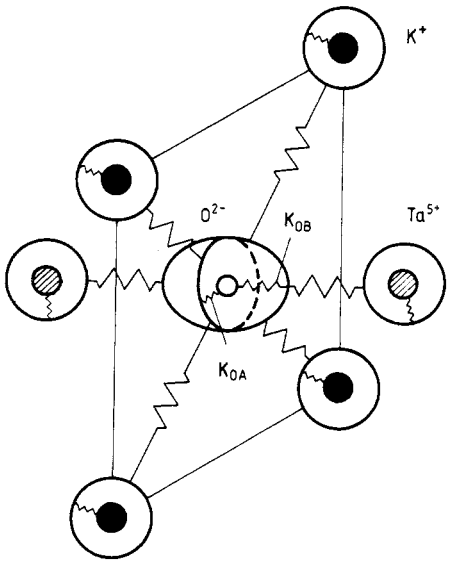

Figure 1. Oxygen and its neighbour ions in the perovskite structure. The ellipsoid at the oxygen site represents the symmetry of its polarisability. The core–shell couplings are isotropic in the case of K^+ and Ta^{5+} ions and anisotropic for the O^{2-} ion. Also indicated are the short-range interactions between the oxygen shell and those of its neighbours.

actions in the model considered are obtained using the harmonic approximation. The effective potential for the shell model is

$$\begin{aligned}\phi = {} & \tfrac{1}{2}\sum_{lki}\sum_{l'k'j}\phi^{s}_{ij}(lk,l'k')v_i(lk)v_j(l'k') + \tfrac{1}{2}\sum_{lki}K_{ki}[u_i(lk)-v_i(lk)]^2 \\ & + \frac{1}{4!}\sum_{lki}K_{\mathrm{OB-B}}\delta_{k\mathrm{O}_i}[u_i(lk)-v_i(lk)]^4 \\ & + \sum_{lki}\sum_{l'k'j}{}' \phi^{c}_{ij}(lk,l'k')\{\tfrac{1}{2}X_kX_{k'}u_i(lk)[u_j(l'k')-u_j(lk)] \\ & + \tfrac{1}{2}Y_kY_{k'}v_i(lk)[v_j(l'k')-v_j(lk)] \\ & + X_kY_{k'}[u_i(lk)v_j(l'k') - \tfrac{1}{2}u_i(lk)u_j(lk) - \tfrac{1}{2}v_i(l'k')v_j(l'k')]\} \qquad (1)\end{aligned}$$

where $\boldsymbol{u}$ and $\boldsymbol{v}$ are the displacements of cores and shells, respectively, from their mean positions in the pure crystal. i denotes Cartesian components; l and k identify unit cells and atomic positions within the cell, respectively. O_i denotes an oxygen whose Ta neighbours lie along the i direction. $\boldsymbol{\phi}^s$ is the short-range force constant matrix between shells, K_{ki} are the core–shell coupling constants and

$$\phi^{c}_{ij}(lk,l'k') = [\partial^2 r^{-1}/(\partial r_i\,\partial r_j)]|_{r=r(lk)-r(l'k')}$$

X_k and Y_k are the core and shell charges, respectively. We shall use Z_k later for the total ionic charge.

The equilibrium conditions for cores is

$$f^{c}_i(lk) \equiv -\partial V(\boldsymbol{u},\boldsymbol{v})/\partial u_i(lk) = \partial\phi/\partial u_i(lk) \qquad (2)$$

and for shells

$$f^{s}_i(lk) \equiv -\partial V(\boldsymbol{u},\boldsymbol{v})/\partial v_i(lk) = \partial\phi/\partial v_i(lk). \qquad (3)$$

For the following treatment it is convenient to write the above equations in terms of

the relative shell–core displacements $\boldsymbol{w} = \boldsymbol{v} - \boldsymbol{u}$. The right-hand sides of equations (2) and (3) are linear in $\boldsymbol{u}$ and $\boldsymbol{w}$ except for the term in equation (3) arising from the fourth-order core–shell interaction at oxygen. This term is considered together with the forces $\boldsymbol{f}^{\mathrm{s}}(lk)$. From the remaining linear terms in equation (3) we solve for the shell variable $\boldsymbol{w}$. This is then replaced in the sum of equations (2) and (3). Finally, the resulting equation is solved for $\boldsymbol{u}$, leading to

$$\boldsymbol{u} = \mathbf{g}\boldsymbol{f}^{\mathrm{t}} - \mathbf{a}\boldsymbol{f}' \tag{4}$$

$$\boldsymbol{w} = \mathbf{b}\boldsymbol{f}' - \mathbf{c}\boldsymbol{u}. \tag{5}$$

The above-described procedure involves force constant matrix inversions which are performed via their Fourier expressions in reciprocal space. In equations (4) and (5), $\boldsymbol{f}^{\mathrm{t}} = \boldsymbol{f}^{\mathrm{s}} + \boldsymbol{f}^{\mathrm{c}}$ contains the total forces exerted by the defect on the lattice ions, and

$$f_i'(lk) = f_i^{\mathrm{s}}(lk) - (1/3!)K_{\mathrm{OB,B}}\delta_{k\mathrm{O}_i}w_i^3(l\mathrm{O}_i). \tag{6}$$

$\mathbf{g}$ is obtained from the dynamical matrix $\mathbf{D}$ of the shell model as follows:

$$g_{ij}(lk, l'k') = \frac{1}{N}\sum_{\boldsymbol{q}} G_{ij}(kk', \boldsymbol{q}) \exp\{\mathrm{i}\boldsymbol{q}\cdot[\boldsymbol{r}(lk) - \boldsymbol{r}(l'k')]\} \tag{7}$$

where $\mathbf{G}(\boldsymbol{q}) = \mathbf{D}^{-1}(\boldsymbol{q})$ with

$$\mathbf{D} = (\mathbf{S} + \mathbf{C}^{zz}) - (\mathbf{S} + \mathbf{C}^{yx})^{\mathrm{T}}(\mathbf{S} + \mathbf{K} + \mathbf{C}^{yy})^{-1}(\mathbf{S} + \mathbf{C}^{yz}). \tag{8}$$

Here $\mathbf{S}$ is the transform of $\boldsymbol{\phi}^{\mathrm{s}}$ and $\mathbf{C}^{zz}$, $\mathbf{C}^{yz}$ and $\mathbf{C}^{yy}$ are the Coulomb force constant matrices in reciprocal space. $\mathbf{K}$ is a diagonal matrix containing the core–shell coupling constants. Analogously to $\mathbf{g}$ in equation (7), the matrices $\mathbf{a}$, $\mathbf{b}$ and $\mathbf{c}$ are obtained from the matrices in reciprocal space:

$$\mathbf{A} = \mathbf{G}(\mathbf{S} + \mathbf{C}^{yz})^{\mathrm{T}}\mathbf{B} \tag{9}$$

$$\mathbf{B} = (\mathbf{S} + \mathbf{K} + \mathbf{C}^{yy})^{-1} \tag{10}$$

$$\mathbf{C} = \mathbf{B}(\mathbf{S} + \mathbf{C}^{yz}). \tag{11}$$

In the limit case where the shells are rigidly displaced with the cores, i.e. $K \to \infty$, the matrix $\mathbf{B}$, and consequently $\mathbf{A}$ and $\mathbf{C}$, vanish and thus $\boldsymbol{u} = \mathbf{g}\boldsymbol{f}^{\mathrm{t}}$. In this case we see that $\mathbf{g}$ is the static lattice Green function for the rigid-ion model.

As is well known, the numerical evaluation of $\mathbf{g}$ from equation (7) depends on the number N of q-points considered in the Brillouin zone. However, it has been shown for an HCP lattice [13] that $\mathbf{g}$ behaves linearly with $1/N$ for sufficiently large N, which allows us to extrapolate $\mathbf{g}$ for infinite N. In the present case, we have found the same linear behaviour. The matrices $\mathbf{b}$ and $\mathbf{c}$ are independent of N, and the matrix $\mathbf{a}$ depends non-linearly but weakly on $1/N$. We have also compared our procedure for the calculation of the Green function with the approach based on the Gilat–Raubenheimer integration method [14]. We found that the latter needs a longer computer time.

The forces $\boldsymbol{f}^{\mathrm{t}}$ and $\boldsymbol{f}'$ in equations (4) and (5) will be evaluated for the core and shell positions in the distorted lattice; hence they are functions of $\boldsymbol{u}$, $\boldsymbol{w}$ and δ. Therefore these are non-linear equations and must be solved self-consistently together with the equilibrium condition for the Li^+ impurity.

Since we are mainly interested in the lattice response for the Li^+ ion displaced along the $\langle 001 \rangle$ direction, as was experimentally observed, we shall restrict the displacement δ to this axis. With this restriction the lithium equilibrium condition is

$$\partial V_{Li}(\boldsymbol{u}, \boldsymbol{w}, \delta)/\partial\delta = -\sum_{lk} f_z^{Li}(lk) = 0. \tag{12}$$

Here $f_z^{Li}(lk)$ are the z components of the short-range and Coulomb forces exerted on the Li by the ion lk.

Li^+ is considered as a rigid ion with the same total ionic charge assigned to K^+ in the model [11]. The Li short-range forces are taken only on nearest-neighbour oxygen shells, as is also the case for K^+ in the host lattice model. Since Li–O potentials of the Born–Mayer type have been previously determined [15, 16], we choose these potentials instead of that used in the aforementioned calculation of the Li displacement [5], which was taken from alkali halide data. The parameters of the potential

$$\varphi(r) = \lambda \exp(-r/\rho) \tag{13}$$

are $\lambda = 1822$ eV and $\rho = 0.2204$ Å, as derived from a study of lattice dynamics in $LiKSO_4$ [15]. From a study of defect energies of Li^+ as substitutes of Ba^{2+} in $BaTiO_3$ a set of parameters $\lambda = 292.3$ eV and $\rho = 0.3472$ Å was obtained [16]. We observe a large difference between both sets of parameters. Since the structure of oxygen ions around Li in $LiKSO_4$ is quite different from that in $KTaO_3$:Li and on the other hand Li^+ substitutes for Ba^{2+} in $BaTiO_3$, thus generating a more complex defect, we do not have *a priori* an argument to choose one of these potentials. Therefore we shall select in section 3 the potential which gives a Li displacement in better agreement with the semiempirical value already determined [5]. The short-range K–O interaction included in the V_K term of the defect potential is chosen to be of the Born–Mayer type, with the parameters determined from the axially symmetric K–O force constants in the shell model.

In order to perform the calculation, the Coulomb forces due to the Li^+ ion and the cancellation of the K^+ ion must be restricted to a finite region around the defect. As considered later, for a reasonable selection of values of the cut-off radius the calculations are not significantly affected by this approximation, since the resulting long-range forces of the defect are of a dipole nature and decay very nearly as $1/r^3$ within a few lattice constants. We wish to point out that the only cut-off imposed on Coulomb interactions is the above-mentioned one, since the long-range interaction between host lattice ions is fully taken into account in the harmonic approximation via the Green functions.

As a result of the cut-off taken for the long-range defect forces, equations (4), (5) and (12) need to be solved only for $\boldsymbol{u}$ and $\boldsymbol{w}$ corresponding to ions within a spherical cluster of the cut-off radius. Note, however, that the influence of the infinite lattice outside the cluster on the displacements inside the cluster is taken into account via the Green functions. The solution for $\boldsymbol{u}$, $\boldsymbol{w}$ and δ is approached by a double iterative procedure, where the perfect lattice positions ($\boldsymbol{u} = \boldsymbol{w} = 0$) and an arbitrary $\delta \neq 0$ are chosen as initial values. For each value of δ, $\boldsymbol{u}$ and $\boldsymbol{w}$ are determined iteratively from equations (4) and (5). This procedure is expected to converge, since $\boldsymbol{u}$ and $\boldsymbol{w}$ on the left-hand sides of equations (4) and (5) arise as the linear response of the system in the configuration adopted in each iteration. Once $\boldsymbol{u}$ and $\boldsymbol{w}$ are thus obtained, a new value of δ is determined from equation (12). The whole iteration is stopped when δ approaches a constant value.

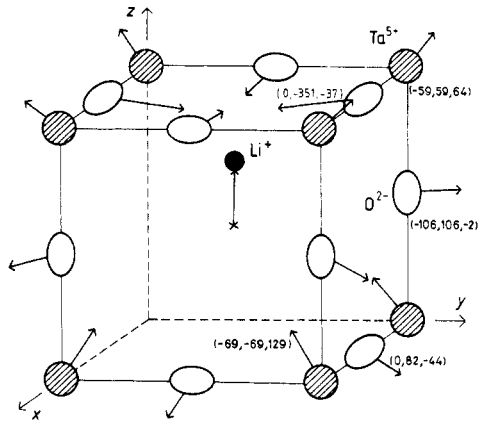

Figure 2. Ionic core displacements of lithium and the tantalum and oxygen neighbours. The Li displacement is in scale with the lattice constant a, and the others are on a ten times greater scale. The values are indicated in units of $10^{-4}a$.

The relaxation volume for the defect will be calculated from the elastic quadrupole tensor $P_{\alpha\beta}$ through the relation

$$\Delta V = (\mathrm{Tr}\, P)/3K \tag{14}$$

where K is the bulk modulus. The quadrupole tensor is obtained as [17]

$$P_{\alpha\beta} = \sum_{lk} [r_\alpha(lk) + u_\alpha(lk)]F^{lk}_\beta(\boldsymbol{r} + \boldsymbol{u}) \tag{15}$$

where $\boldsymbol{F}^{lk}$ is

$$\boldsymbol{F}^{lk} = (\boldsymbol{f}^{\mathrm{t}} - \mathbf{c}^{\mathrm{T}}\boldsymbol{f}'). \tag{16}$$

This force results from equation (4) written in the form $\boldsymbol{u} = \mathbf{g}\boldsymbol{F}$. The second term in equation (16) is the force due to the shell displacements produced by the defect.

3. Results and discussion

A radius R_c of the spherical cluster has to be determined in order that cluster size effects do not affect significantly the results. For this purpose, several R_c-values have been tested. For $R_c \leqslant 2.5a$, the lattice distortion is strongly size dependent. On the other hand, for $R_c = 2.8a$ and $3.1a$, very similar results are obtained. Therefore we shall describe the results corresponding to the latter radius, which includes 122 K^+ ions, 136 Ta^{5+} ions and 408 O^{2-} ions.

As expected, the iteration procedure converges fairly well for both Li–O potentials used. In the case of the potential taken from $BaTiO_3$:Li the equilibrium postion of Li in $KTaO_3$:Li is centrosymmetric. On the other hand, with the other potential the Li displacement converges to the equilibrium value $\delta = 0.36a$, which is in satisfactory agreement with the semiempirical value [5]. Therefore we shall discuss the results obtained with the latter potential.

In the following discussion we shall distinguish between three contributions to the electric dipole moment of the system. First, there is the defect dipole moment produced by the off-centre substitution of Li for K. In addition the host crystal ions give rise to an ionic and an electronic contribution: the first contribution $Z_k\boldsymbol{u}(lk)$ corresponds to the

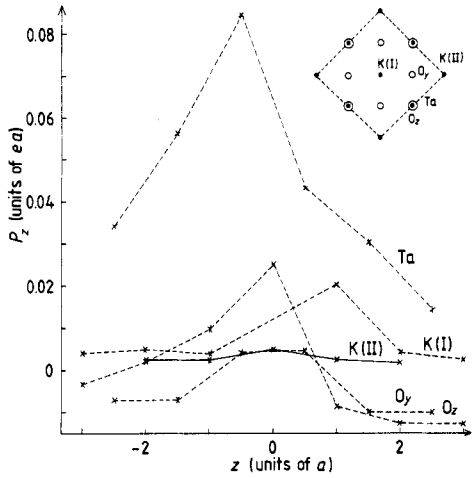

Figure 3. The z component of the total dipole moments of ions along chains parallel to z axis, whose projections are shown in the inset. The abscissa values are the z coordinates in units of a, measured from the Li plane.

core displacements from their equilibrium positions in the pure crystal, and the second contribution $Y_k w(lk)$ is due to the relative shell–core displacement. The displacements of Li neighbour ions are depicted in figure 2. It is clearly seen that the ions are displaced in such a way that each reinforces the defect dipole moment in the z direction. In addition, the electronic polarisation of the Ta and O_z ions makes an important contribution to the z component of the dipole moment. These findings indicate that the total dipole moment in a region around Li is larger than the defect dipole moment. We shall call this polarised region the 'effective dipole'. From the numerical results it is immediately apparent that this region is strongly anisotropic, with its major axis along z. Therefore it is convenient to consider the orientation of dipole moments (ionic plus electronic) in ionic chains parallel to the z axis. Moving away from Li perpendicular to the z direction it is found that the only chains which reinforce the defect dipole moment are those whose positions are indicated in the inset of figure 3. The z components of the total dipole moments of ions along these chains are represented in figure 3. All ions in more distant chains screen the defect dipole moment, except for the negligible contributions of K^+ ions.

To determine the extension of the 'effective dipole' in the z direction, we move along the z direction in both senses from the Li position with a lattice constant step in order to avoid uneven contributions from isolated ions. The 'effective dipole' is considered to end when a given step contributes a screening polarisation. In this way we find the 'effective dipole' schematically represented in figure 4. This extends two unit cells above the Li plane and three unit cells below it. However, this extension may be underestimated because the cluster radius is only $3.1a$. We observed a weak tendency of the polarised region to grow in the longer dimension when increasing R_c from $2.8a$ to $3.1a$. The total dipole moment, including the defect dipole, exceeds about five times the defect dipole moment; more precisely $P_{\text{eff}} = 4.5P_{\text{Li}}$. The Li dipole and the four nearest chains Ta–O_z bear 99% of the 'effective dipole' polarisation.

Regarding the electronic part of the polarisation, it is observed that all potassium shells, and the shells of Ta and O_z ions outside the Ta–O_z chains nearest to the defect, polarise following the defect dipole field. For the ions on the four nearest Ta–O_z chains the electronic polarisation is significantly larger than for the rest of the ions and reinforce

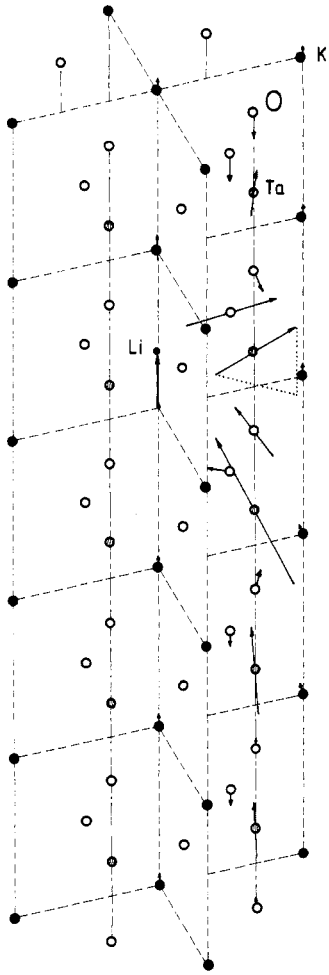

Figure 4. Schematic representation (on an arbitrary scale) of the ionic dipole moments in the effective dipole created around the off-centre lithium.

the defect dipole moment. This reinforcing effect is observed also in the ionic polarisation of Ta ions on those chains, while the ionic contribution of the O_z ions in general screens the defect dipole. The incipient crystal instability of $KTaO_3$ with respect to the ferroelectric mode appears to be reflected in the pattern of lattice dipoles, in particular below the Li position (see figure 4). We notice the remarkable fact that the Ta–O_z chain neighbours to Li polarise against the defect dipole field. First, a trivial calculation shows that the Coulomb forces exerted by the defect on the nearest Ta and O ions are very different from those that would result if the defect were considered as a point dipole. Moreover, the core and shell displacements for these ions do not point in the directions of the Coulomb forces. In fact the defect forces act together with those due to the host ion displacements. As a result of this non-trivial force balance, the defect neighbour ions (shown in figure 2) polarise to reinforce the defect dipole. On the other hand the Lorentz factors for the coupling of ions along a Ta–O_z chain are much larger than for the other pair of ions. As a consequence, ions along these chains tend to polarise in the same sense, with a longer correlation than in the other directions. Thus the anisotropic shape of the 'effective dipole' has the same origin as the correlation volume [18]. An

analogous anisotropic shape was obtained in the previous calculation [5], but contrary to the present results the induced dipoles screened the defect dipole completely. Thus, they do not form an 'effective dipole'. This discrepancy may be assigned to the fact that in our shell model the ionic and electronic polarisation is due not only to Coulomb forces, as in the previous work [5], but also to short-range forces between shells, which correlate neighbour ion displacements.

The Li displacement δ can also be estimated in our model framework from the quadrupole coupling frequency ν_Q determined by NMR techniques. ν_Q is related to the electric field gradient V_{zz} at the Li position as explained in [5]. We calculate V_{zz} for different values of δ by adding directly the contribution of ions in their relaxed lattice positions in the sphere of radius $3.1a$ and taking into account also ions in their perfect lattice positions up to a radius of $10a$. The Li displacement which corresponds to the measured $\nu_Q = 70 \pm 3$ kHz is $\delta = 0.30a$. This value is in reasonable agreement with the displacement obtained from the potential energy minimum of the shell model, although the discrepancy is larger than in the calculation with the polarisable point charge model [5].

In contrast to the large extension of the electric displacement induced by the impurity, ultrasonic attenuation measurements allowed us to determine a volume per impurity of $0.0026a^3$ [19], which characterises a small spatial range of mismatch at the impurity site. Calculating the components of the elastic quadrupole tensor according to equation (15), we obtain the values $P_{xx} = P_{yy} = -2.08$ eV and $P_{zz} = -2.38$ eV and the remaining components are zero. With the bulk modulus corresponding to the model elastic constants [11], $K = 1.34 \times 10^{24}$ eV cm^{-3}, the relaxation volume results from equation (14): $\Delta V = -0.0025a^3$. This indicates that an average inward relaxation of the lattice occurs. This is in excellent agreement with the value obtained in [19], taking into account the fact that those measurements did not allow determination of the sign of ΔV.

For the effective harmonic core–shell coupling constant $K_{OB}(T)$ at the oxygen atom, we have taken the room-temperature value $357.5e^2/a^3$ [11]. However, by testing values of $K_{OB}(T)$ which fit the ferroelectric soft mode of pure $KTaO_3$ at several temperatures, no significant changes in the results are observed. Moreover the calculated distortions are almost not affected by the suppression of the w^3 term in equation (6). This means that the appearance of an 'effective dipole' is essentially a property of the harmonic crystal. On the other hand, precise assessment of temperature effects on the distortions deserves a more careful treatment of the anharmonic properties in the defect crystal.

Summarising, with a model which has been proved to be capable of describing several dynamical properties of pure $KTaO_3$, and with a Li–O interaction potential which leads to a Li displacement compatible with experimental observations, we obtain a polarised region reinforcing the Li dipole moment. This is in agreement with the experimental fact that the off-centre Li ion cannot be solely responsible for the observed polarisation effects [6–8].

Acknowledgments

We acknowledge support from the Consejo Nacional de Investigaciones Científicas y Técnicas. We are grateful to Dr U T Höchli for suggesting this research and for his helpful information. We thank A Dobry and A Greco for helpful discussions.

References

[1] Yacoby Y and Just S 1974 *Solid State Commun.* **15** 715
[2] Borsa F, Höchli U, van der Klink J J and Rytz D 1980 *Phys. Rev. Lett.* **45** 1884
[3] Yacoby Y 1981 *Z. Phys.* B **41** 269
[4] van der Klink J J, Rytz D, Borsa F and Höchli U 1983 *Phys. Rev.* B **27** 89
[5] van der Klink J J and Khanna S 1984 *Phys. Rev.* B **29** 2415
[6] Höchli U and Baeriswyl D 1984 *J. Phys. C: Solid State Phys.* **17** 311
[7] Höchli U, Weibel H and Boatner L 1979 *J. Phys. C: Solid State Phys.* **12** L563
[8] Vugmeĭster B, Glinchuk M and Pechenyĭ A 1984 *Sov. Phys.–Solid State* **26** 2036
[9] Vugmeĭster B, Glinchuk M and Pechenyĭ A 1985 *Ferroelectrics* **64** 1
[10] Kleemann W, Kütz S and Schäfer F 1988 *Phys. Rev.* B **37** 5856
[11] Perry C, Currat R, Buhay H, Migoni R, Stirling W and Axe J 1989 *Phys. Rev.* B **39** 8666
[12] Bilz H, Benedek G and Bussmann-Holder A 1987 *Phys. Rev.* B **35** 4840
[13] Migoni R, Tomé C, Smetniansky-De Grande N and Savino E 1980 *Phys. Rev.* B **22** 2658
[14] Schober H, Mostoller M and Dederichs P 1974 *Phys. Status Solidi* b **64** 173
[15] Chaplot S and Rao K 1987 *Phys. Rev.* B **35** 9771
[16] Lewis G and Catlow C 1986 *J. Phys. Chem. Solids* **47** 89
[17] Schober H and Ingle K 1980 *J. Phys. F: Met. Phys.* **10** 575
[18] Wemple S, Di Domenico M and Jayaraman A 1969 *Phys. Rev.* **180** 547
[19] Höchli U T, Weibel H E and Rehwald W 1982 *J. Phys. C: Solid State Phys.* **15** 6129